Direct observation of grain growth from molten silicon formed by micro-thermal-plasma-jet irradiation

Shohei Hayashi,[a] Yuji Fujita, Takahiro Kamikura, Kohei Sakaike, Muneki Akazawa, Mitsuhisa Ikeda, Hiroaki Hanafusa, and Seiichiro Higashi[b]
Department of Semiconductor Electronics and Integration Science, Graduate School of Advanced Sciences of Matter, Hiroshima University, 1-3-1 Kagamiyama, Higashi-Hiroshima, Hiroshima 739-8530, Japan

(Received 2 September 2012; accepted 12 October 2012; published online 26 October 2012)

Phase transformation of amorphous-silicon during millisecond annealing using micro-thermal-plasma-jet irradiation was directly observed using a high-speed camera with microsecond time resolution. An oval-shaped molten-silicon region adjacent to the solid phase crystallization region was clearly observed, followed by lateral large grain growth perpendicular to a liquid-solid interface. Furthermore, leading wave crystallization (LWC), which showed intermittent explosive crystallization, was discovered in front of the moving molten region. The growth mechanism of LWC has been investigated on the basis of numerical simulation implementing explosive movement of a thin liquid layer driven by released latent heat diffusion in a lateral direction. © *2012 American Institute of Physics*. [http://dx.doi.org/10.1063/1.4764522]

The crystallization of amorphous silicon (a-Si) films on glass substrates is a key process technology in the fabrication of large-area electronic devices such as solar cells and thin-film transistors (TFTs). Various crystallization technologies have been extensively studied to form high-crystallinity Si films.[1–6] To improve device performance and uniformity, grain growth mechanism during rapid thermal annealing (RTA) and the control of grain structures including location and orientation have been investigated. Additionally, various measurement techniques have been proposed for observing phase transformation of Si films.[4–12] Transient reflectance (TR) measurements during RTA enable observation of the phase transformation of Si film since molten Si has much higher reflectivity than that of solid Si.[4–10] Transient conductance (TC) measurement makes it possible to obtain the volume of molten Si and liquid-solid interface velocity.[4–9] The TR and TC measurements indicated that partial or complete melting was induced directly from a–Si films by laser irradiation. Either microcrystallization or amorphization is induced after the complete melting of a Si film.[6] Moreover, it was clarified that extremely fast movement of a thin liquid layer and the resulting fine grain crystalline formation, known as "explosive crystallization (EC)," take place when pulsed-laser irradiation of a-Si is performed under partially melted conditions.[7–10] Large latent heat is produced by the phase transformation from an amorphous to a crystalline state as reported after conducting differential scanning calorimeter (DSC) measurement.[11] The DSC measurement indicated a melting point of a-Si of 1420 K, which is lower than that of crystalline Si (c-Si), and made it possible to measure the value of the molar enthalpy of crystallization. The EC induced in the lateral direction has been proposed at the continuous-wave (CW) laser crystallization within a period of milliseconds,[12] but its phase transformation has not been directly observed.

In our previous work, the application of an atmospheric pressure DC arc discharge micro-thermal-plasma-jet (μ-TPJ) was proposed for crystallization of amorphous Si (a-Si) films within a period from microseconds to milliseconds.[13–16] TR measurement during μ-TPJ irradiation indicated that solid phase crystallization (SPC) took place prior to the formation of a molten region (MR).[14,15] High-speed lateral crystallization (HSLC) is induced by moving the MR at very high speed to form a lateral temperature gradient, which results in the growth of large grains of roughly 60 μm. TFTs fabricated by HSLC-Si films showed a very high field-effect mobility (μ_{FE}) of 477 $cm^2\ V^{-1}\ s^{-1}$.[16] However, our understanding of the grain growth mechanism is still insufficient, and investigation of the crystallization mechanism is very important for application to high performance and uniform devices. In this letter, we introduce a microsecond-time-resolving high-speed camera (HSC) for direct observation of phase transformation. Observation of intermittent lateral crystal growth in SPC film and its mechanism are discussed.

Amorphous Si films were formed on quartz substrates by plasma-enhanced chemical vapor deposition (PECVD) using SiH_4 and H_2 at 250 °C. The thickness of the a-Si films was varied from 50 to 500 nm. Dehydrogenation was carried out at 450 °C in N_2 ambient for 1 h. μ-TPJ was generated by DC arc discharge under atmospheric pressure with a supplying power (P) of 0.8–1.7 kW between a W cathode and Cu anode separated by 2.0 mm. The Ar gas flow rate (f) was varied from 1.0 to 4.2 l/min. μ-TPJ was formed by blowing out the thermal plasma through an orifice with a diameter of 600 μm. The substrate was linearly moved by a motion stage in front of the μ-TPJ with a scanning speed (v) ranging from 500 to 2000 mm/s. The distance between the plasma source and substrate (d) was varied from 1.0 to 1.5 mm. For the *in-situ* observation of grain growth of a-Si films during μ-TPJ irradiation, an optical microscope and a HSC were set on the motion stage on the backside of the substrate. The frame-rate (R_f) was varied from 3000 to 165 000 frames per second (fps).

Phase transformation of 100-nm-thick Si film during μ-TPJ irradiation was very clearly observed, as in the

[a]Research Fellow of the Japan Society for the Promotion of Science.
[b]Electronic mail: semicon@hiroshima-u.ac.jp.

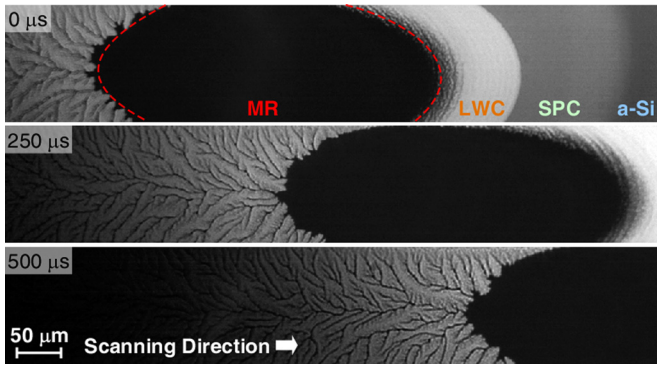

FIG. 1. HSC snapshots of moving MR and subsequent lateral crystallization in 100-nm-thick Si film taken by HSC at $R_f = 16\,000$ fps during μ-TPJ irradiation. TPJ irradiation conditions were $P = 1.1$ kW, $d = 1.5$ mm, $f = 2.8$ L/min, and $v = 800$ mm/s.

snapshots shown in Fig. 1. Because liquid Si shows very high reflectivity due to free carriers, the MR can be seen in black surrounded by red dotted lines in Fig. 1. A SPC region formed in front of the molten Si was clearly distinguished from the amorphous phase. These results agree with the results of TR measurement during μ-TPJ irradiation in our previous work.[14,15] Following the movement of MR, grains grew perpendicularly to a liquid-solid interface. It should be noted that a region showing a wave-like pattern exists between the MR and SPC regions. The obviously different contrast and pattern suggest a completely unknown crystallization mechanism. We call this "leading wave crystallization (LWC)" because it exhibits a periodic and repeating structure like waves.

To better understand the behavior of LWC, HSC images were taken during μ-TPJ irradiation of $t_{Si} = 100$–500-nm-thick Si films (Fig. 2). With the increase in t_{Si}, the length of the LWC period (L_{LWC}) increased from 15 to 70 μm. The increase in L_{LWC} with thickness suggests that in addition to heat conducted from μ-TPJ, latent heat also plays a very important role in LWC. HSC images during μ-TPJ irradiation of 500-nm-thick Si film taken at a very high R_f of 27 000 fps are shown in Fig. 3. The MR moves at a constant speed, which is identical to $v = 650$ mm/s. On the contrary, the LWC front remained in the same position from 0 to 37 μs, then suddenly moved to ~66 μm at 74 μs. Again, LWC did not occur from 74 to 148 μs, and then explosive grain growth occurred again between 148 and 185 μs. From higher time-

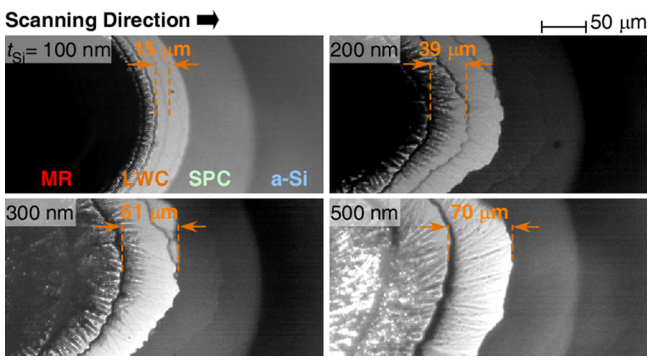

FIG. 2. HSC snapshots focusing on LWC regions of Si film during μ-TPJ irradiation to 100–500-nm-thick a-Si films under condition of $P = 1.4$ kW, $d = 1.0$ mm, $f = 2.0$ l/min, and $v = 1500$ mm/s.

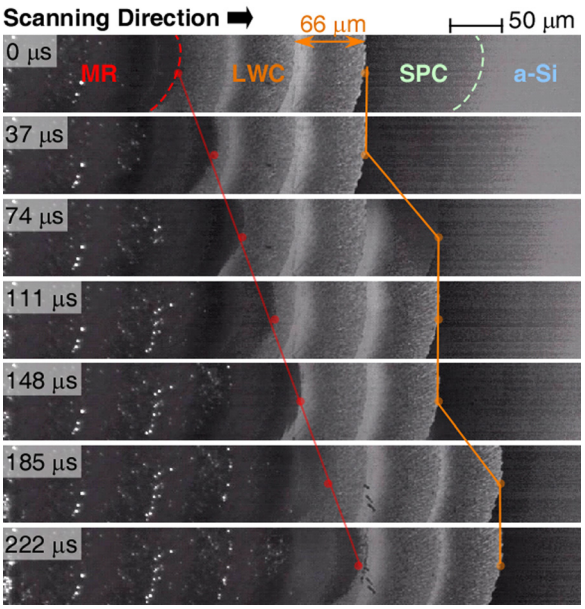

FIG. 3. HSC snapshots of Si film taken at $R_f = 27\,000$ fps during μ-TPJ irradiation ($P = 1.3$ kW, $d = 1.5$ mm, $f = 1.5$ l/min, $v = 650$ mm/s) of 500-nm-thick a-Si films.

resolved observation of $R_f = 165\,000$ fps, LWC propagation velocity was measured to be high as 4500 mm/s, which is significantly faster than v. These results indicate that LWC is quite similar to EC. However, previous reports claim that the driving force of EC is the released latent heat at the liquid-amorphous interface.[7–10,12] In the present case, EC propagates into the SPC region, which obviously has less latent heat. To confirm this, μ-TPJ irradiation of a-Si film was first carried out to form SPC and HSLC regions, and a second irradiation was done with the films under HSC observation. In the HSLC-Si region, which had large lateral grains, no formation of a LWC region was observed, as shown in Fig. 4(a). On the contrary, we clearly observed LWC after the second μ-TPJ irradiation of the SPC-Si film, as shown in Fig. 4(b). This result suggests that sufficient latent heat remains in the SPC region, and the melting point of SPC-Si (T_{SPC}) is lower than that of crystalline Si (T_C). This presumably triggers the formation of a liquid layer, and then extremely fast propagation of this layer into the SPC region is driven by released latent heat. HSLC-Si films showed a crystalline volume fraction of 100% from Raman scattering spectra, while that of SPC was 50%–60%. This suggests that a substantial amount of a disordered structure or amorphous component remains in the SPC region.

The following crystallization model of one LWC period was applied (Fig. 5), and numerical calculations were conducted in order to explain the experimental results quantitatively. A thin liquid Si layer (l-Si) is formed when SPC-Si reaches the T_{SPC} by heat conducted from μ-TPJ (Fig. 5(b)). T_{SPC} is determined by the crystal volume fraction of SPC-Si film (R_C). $T_{SPC} = 1420$ and 1687 K are assumed for $R_C = 0\%$ and 100%, respectively,[12] and it is also assumed that T_{SPC} linearly increase with the increasing R_C. Very high-speed movement of l-Si is driven by undercooling (ΔT).[17,18] Latent heat of 50.7 kJ/mol is produced by phase transformation from liquid to solid (H_{LC}),[11] and heat diffusions from l-Si to

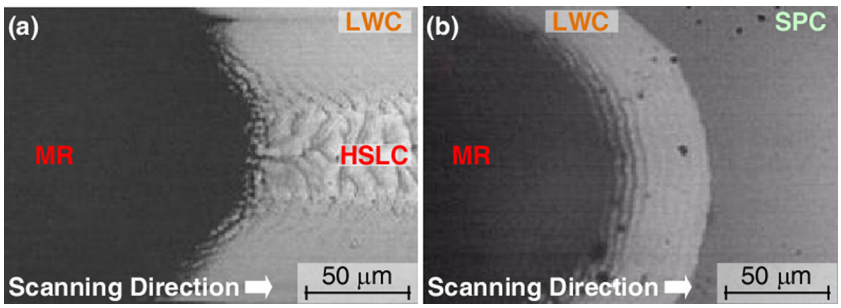

FIG. 4. HSC snapshots of Si film during second μ-TPJ irradiation under HSLC conditions ($P = 1.3$ kW, $d = 1.5$ mm, $f = 1.0$ l/min, and $v = 600$ mm/s) of 100-nm-thick (a) HSLC and (b) SPC-Si films.

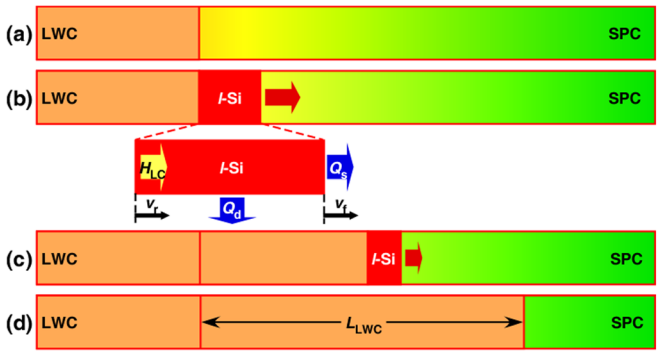

FIG. 5. Schematic of LWC generation model. A thin liquid layer explosively driven in scanning direction has been implemented.

scanning direction (Q_s) and substrate underneath (Q_d) are taken into account. Q is the heat used to increase the temperature of the next SPC region to T_{SPC}, and H_{SPCL} is the absorbed latent heat at phase transformation from SPC to liquid. Here, H_{LC}, H_{SPCL}, Q_s, and Q_d are defined in units of lateral length, and T_{SPC} and H_{SPCL} were independently determined based on R_C. The ΔT is written as

$$\Delta T = T_C - T_{SPC}. \tag{1}$$

An equation of the heat balance is shown in

$$H_{LC} t_{Si} L_r - (Q_s + Q_d) = H_{SPCL} L_f t_{Si} + Q, \tag{2}$$

$$Q_s = \kappa_{Si} t_{Si} \frac{\partial T}{\partial x_s}, \tag{3}$$

$$Q_d = \kappa_Q L_r \frac{\partial T}{\partial x_d}. \tag{4}$$

Here, L_f and L_r are melting and solidification length in unit time step (t), κ_{Si} and κ_Q are thermal conductivity of solid Si and quartz, respectively. The temperature gradient is determined by the thermal diffusion length (L_D). L_D is obtained by the following equation:

$$L_D = \sqrt{Dt}, \tag{5}$$

$$\frac{\partial T}{\partial x} = \frac{T_D - T_{SPC}}{L_D}. \tag{6}$$

Here, D is thermal diffusivity, and T_d is temperature at the position diffused from the front of l-Si, respectively. The dependences of κ_{Si}, κ_Q, and D on temperature are also taken into consideration. The velocity of the front interface of l-Si (v_f) propagating into the SPC region at very high speed was determined based on L_f and time. Q_s, Q_d, and Q increase with propagation of the front interface of l-Si due to the increasing temperature gradient. Therefore, v_f decreases with the propagation of l-Si. In contrast, the rear interface velocity (v_r) of l-Si, which is determined by ΔT,[17,18] is assumed to be constant. As a result, the rear interface overtakes the front interface of l-Si, and LWC propagation terminates with the disappearance of l-Si. The next LWC period starts again when SPC regions are melted by heat conducted from μ-TPJ. The intermittent growth is induced because these processes occur repeatedly. To estimate the temperature of Si film during μ-TPJ irradiation, thermal diffusion simulation was carried out on the basis of a two-dimensional heat diffusion simulation reported previously.[19] From the calculation, L_{LWC} values were estimated and compared with the experimental results as shown in Fig. 6. The experimental results are well reproduced based on the proposed model. These results indicate that the increase in H_{LC} with the increase in t_{Si} leads to the expansion of L_{LWC}. Then, 500-nm-thick a-Si films were crystallized under the condition of $v = 600$–1500 mm/s, and the increasing L_{LWC} with v was clearly observed. Temperature analysis carried out in a thermal diffusion simulation[19] clarified that the temperature gradient at the front of the MR decreased as v increased. Therefore, Q_s, Q_d, and Q decrease with the increasing v. In addition, Raman scattering spectra showed that R_C decreased as v increased. As a result, L_{LWC} expanded with the increasing v, and the simulated L_{LWC} corresponded with the experimental results

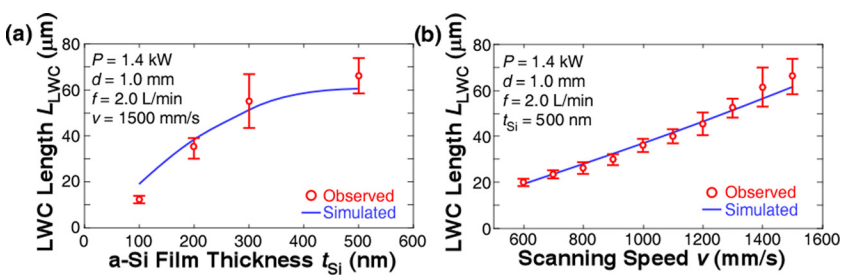

FIG. 6. L_{LWC} dependence on (a) t_{Si} and (b) v obtained experimentally and simulated using the model shown in Fig. 5.

(Fig. 6(b)). These results indicate that the proposed model includes the basic LWC mechanism.

A part of this work was supported by the Research Institute for Nanodevice and Bio Systems (RNBS) and the Natural Science Center for Basic Research and Development (N-BARD), Hiroshima University. A part of this work was supported by the Funding Program for Next Generation World-Leading Researchers (NEXT Program) from the Japan Society for the Promotion of Science (JSPS).

[1]S. W. Lee and S. K. Joo, IEEE Electron Device Lett. **17**, 160 (1996).
[2]A. Hara, M. Takei, F. Takeuchi, K. Suga, K. Yoshino, M. Chida, T. Kakehi, Y. Ebiko, Y. Sano, and N. Sasaki, Jpn. J. Appl. Phys. Part 1 **43**, 1269 (2004).
[3]T. Noguchi, Y. Chen, T. Miyahira, J. D. Mugiraneza, Y. Ogino, Y. Iida, and M. Terao, Jpn. J. Appl. Phys. Part 1 **49**, 03CA10 (2010).
[4]T. Sameshima and S. Usui, J. Appl. Phys. **70**, 1281 (1991).
[5]M. Hatano, S. Moon, M. Lee, K. Suzuki, and C. P. Grigoropoulos, J. Appl. Phys. **87**, 36 (2000).
[6]S. Higashi and T. Sameshima, Jpn. J. Appl. Phys. Part 1 **40**, 480 (2001).
[7]M. O. Thompson, G. J. Galvin, J. W. Mayer, P. S. Peercy, J. M. Poate, D. C. Jacobson, A. G. Cullis, and N. G. Chew, Phys. Rev. Lett. **52**, 2360 (1984).
[8]H. D. Geiler, E. Glaser, G. Gotz, and M. Wagner, J. Appl. Phys. **59**, 3091 (1986).
[9]S. R. Stiffler and M. O. Thompson, Phys. Rev. Lett. **60**, 2519 (1988).
[10]K. Murakami, O. Eryu, K. Takita, and K. Masuda, Phys. Rev. Lett. **59**, 2203 (1987).
[11]E. P. Donovan, F. Spaepen, D. Turnbull, J. M. Poate, and D. C. Jacobson, Appl. Phys. Lett. **42**, 698 (1983).
[12]D. Bensahel, G. Auvert, A. Perio, and J. C. Pfister, J. Appl. Phys. **54**(6), 3485 (1983).
[13]H. Kaku, S. Higashi, H. Taniguchi, H. Murakami, and S. Miyazaki, Appl. Surf. Sci. **244**, 8 (2005).
[14]S. Hayashi, S. Higashi, H. Murakami, and S. Miyazaki, Appl. Phys. Express **3**, 061401 (2010).
[15]S. Higashi, S. Hayashi, Y. Hiroshige, Y. Nishida, H. Murakami, and S. Miyazaki, Jpn. J. Appl. Phys. Part 1 **50**, 03CB10 (2011).
[16]Y. Fujita, S. Hayashi, and S. Higashi, Jpn. J. Appl. Phys. Part 1 **51**, 02BH05 (2012).
[17]C. Panofen and D. M. Herlach, Appl. Phys. Lett. **88**, 171913 (2006).
[18]J. Lipton, W. Kurz, and R. Trivedi, Acta Metall. **35**, 957 (1987).
[19]T. Okada, S. Higashi, H. Kaku, N. Koba, H. Murakami, and S. Miyazaki, Jpn. J. Appl. Phys. Part 1 **45**, 4355 (2006).